Supplement of Atmos. Chem. Phys., 25, 741–758, 2025
https://doi.org/10.5194/acp-25-741-2025-supplement
© Author(s) 2025. CC BY 4.0 License.

Atmospheric Chemistry and Physics
Open Access
EGU

Supplement of

External particle mixing influences hygroscopicity in a sub-urban area

Shravan Deshmukh et al.

Correspondence to: Shravan Deshmukh (deshmukh@tropos.de), Laurent Poulain (poulain@tropos.de), and Mira Pöhlker (poehlker@tropos.de)

The copyright of individual parts of the supplement might differ from the article licence.

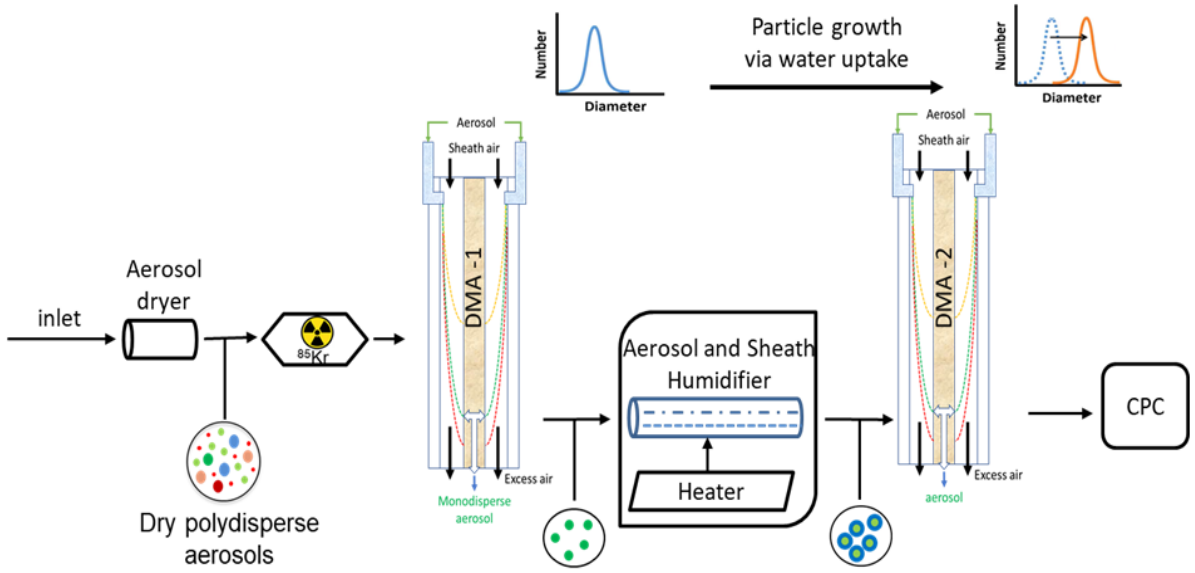

855 **Figure S1. Schematic diagram of the TROPOS made - HTDMA system.**

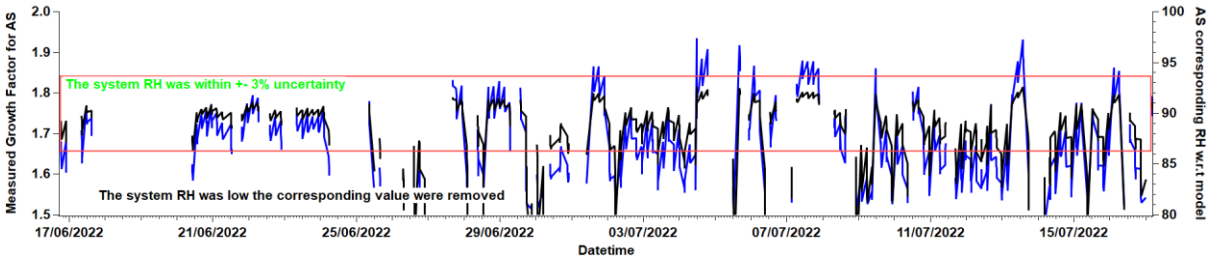

860 **Figure S2. Ammonium sulphate (AS) calibration time series during the campaign using the HTDMA system. The corresponding RH for AS from the EPS model and TDMAinv toolkit by Gysel is on the right axis.**

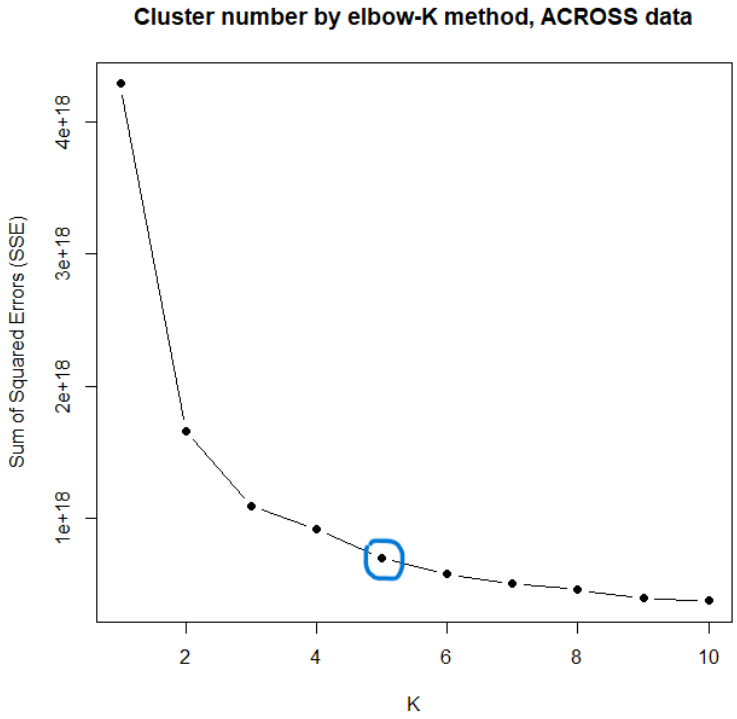

Figure S3. Calculated cluster number using elbow-K mean method.

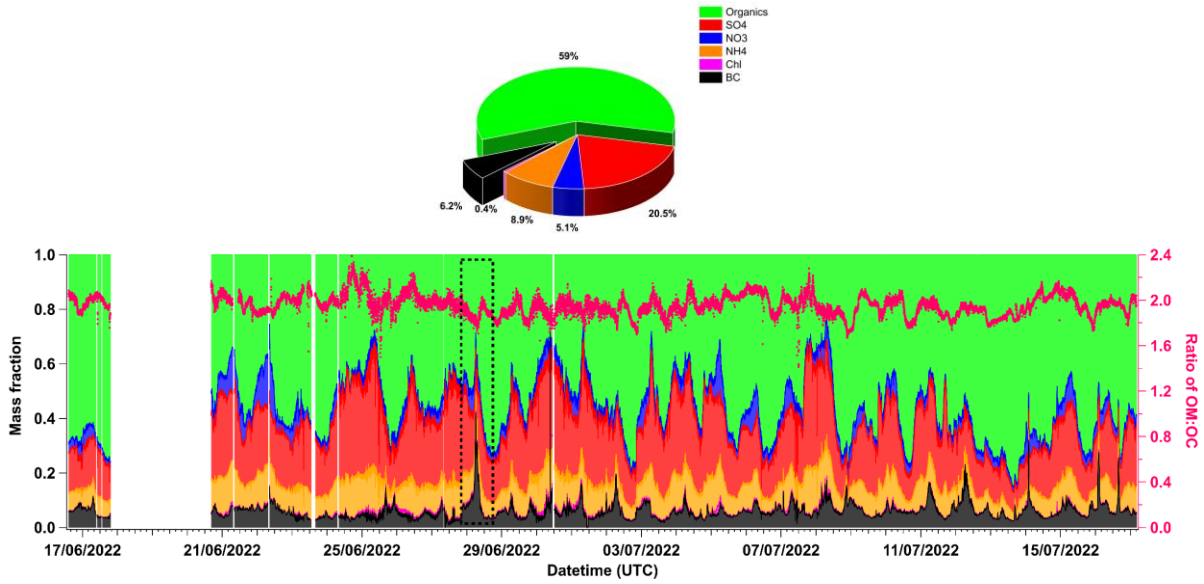

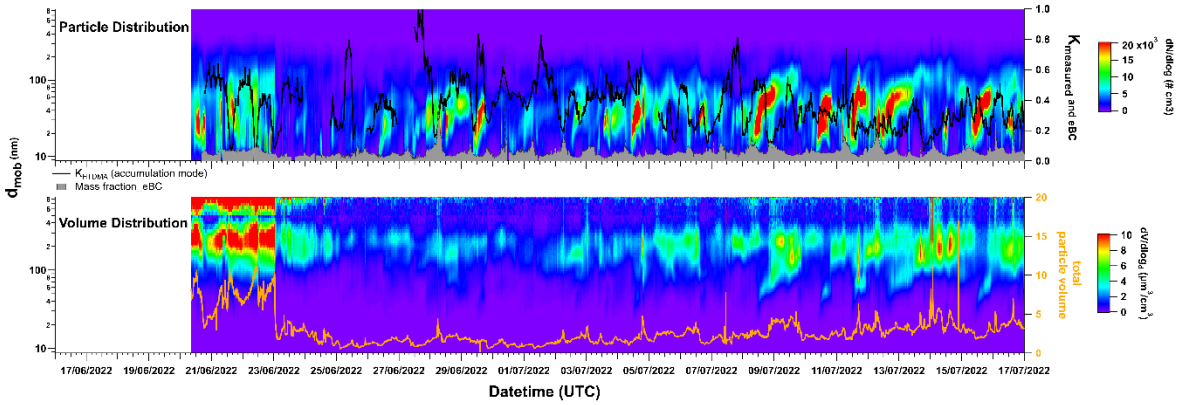

Figure S4. Mass spectra from AMS, with time series and mass fraction (a); the timeseries of PNSD and volume distribution with Kappa and eBC (b).

Several events were encountered during the campaign, including high Particulate Matter (PM) mass concentration in the initial period with the first heatwave and temperatures close to 40° C. The total contribution of organics was higher than that of other constituents. The SO4 peaks seen during the campaign were thought to be attributed to either industrial emissions in Rouen (Northern side of Paris) or shipping emissions in the channel - Le Havre region, from Fig. 1. This could be attributed to NW winds. The OM (organic matter) and OC ratios varied, sharply dropping when a BC peak or rise occurred. Some burning plume events are encountered in the close vicinity of the measuring site.

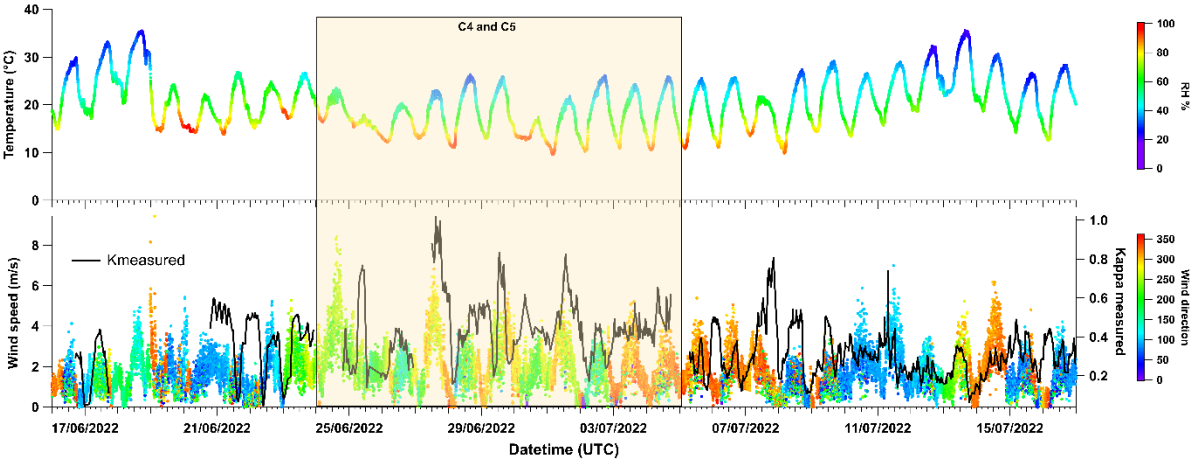

Figure S5. Meteorological temporal variation.

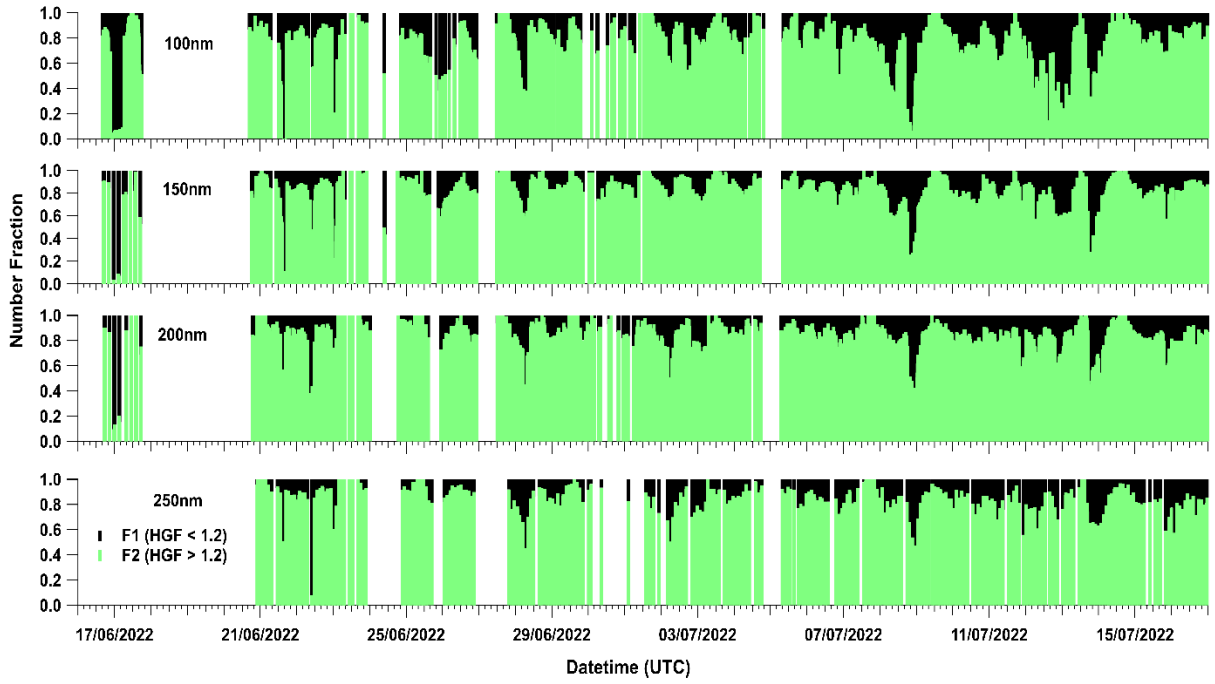

Figure S6. Number fraction for all diameters, where F1 is GF<1.2, and F2 is GF>1.2.

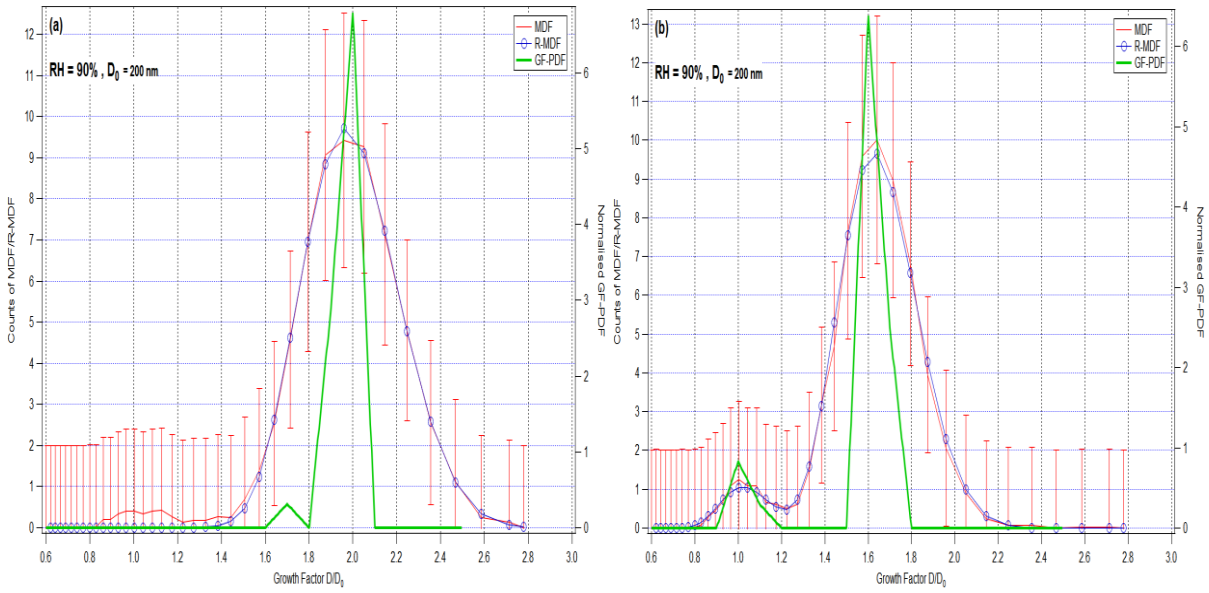

Figure S7. Example of growth factor distributions measured at RH = 90 % of D_0 = 200 nm particles (a, internally mixed) and (b, externally mixed with distinct modes). The red line represents the measured particle counts, the blue line represents the reconstructed measured distribution function, and the green line is the GF-PDF.

The GF standard deviation or sigma (σ) of a GF-PDF was determined according to Eq. (C.6) in Gysel et al. (2009). The categorization or grouping is used to identify the modes in GF-PDF for all scans for all diameters over time. The number of modes of GF-PDF was considered to be the identification of sigma values over time series. Mode equal to 1 represents internally mixed particles, and most of the σ values associated with single mode are below 0.08 and above is associated with large sigma and externally mixed particles. Grouping of σ in the present study is also used as a reference from (Sjogren et al., 2008 and C. Spitieri et al., 2023).

GF-PDF equation for corrected GF by (Sjogren et al., 2008)

$$\kappa(GF, aw) = \frac{(GF^3 - 1)(1 - a_\omega)}{a_\omega}$$

$$GF(\, aw, \kappa\,) = \left(1 + k\frac{a_\omega}{1 - a\omega}\right)^{1/3}$$

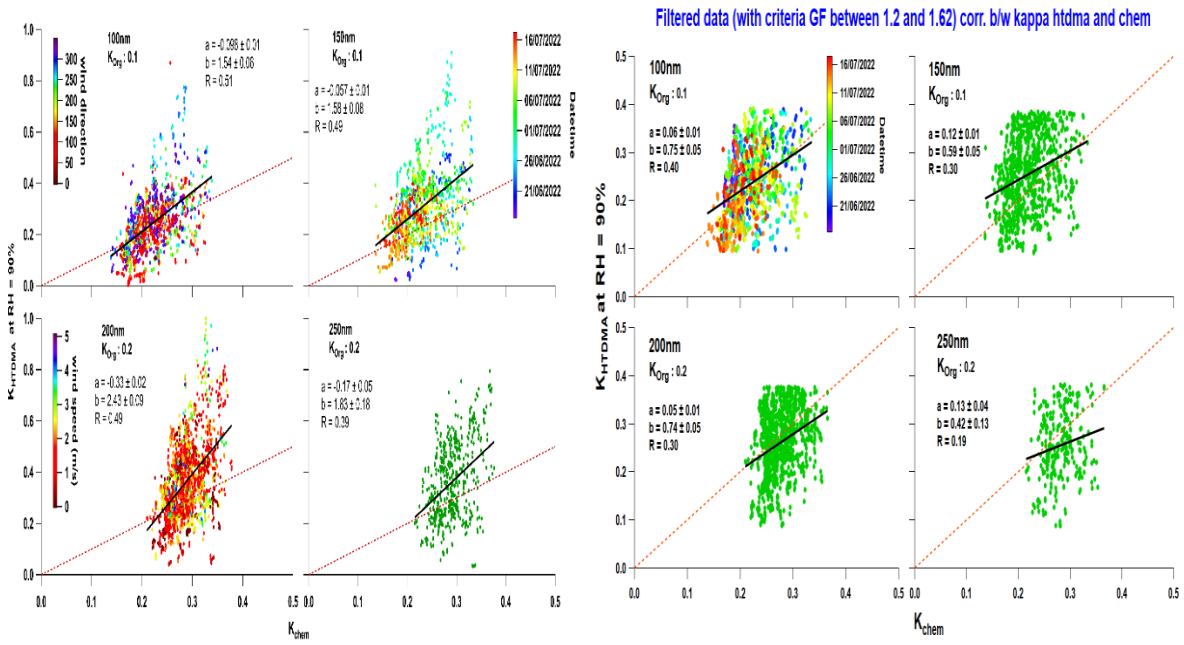

Figure S8. Correlation between measured kappa (κ_{HTDMA}) and predicted kappa (κ_{chem}) for all sizes with and without filter/segregated.

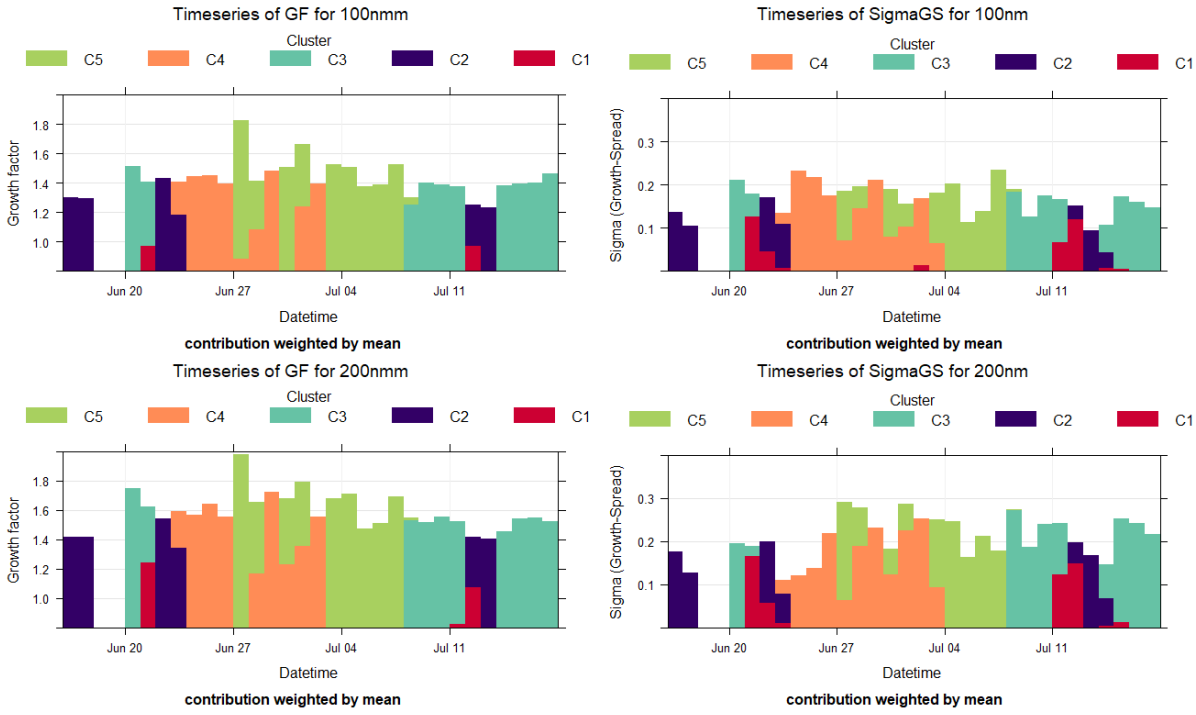

Figure S9. Time prop contribution of clusters with Growth factor and Chemical composition for 100 and 200nm

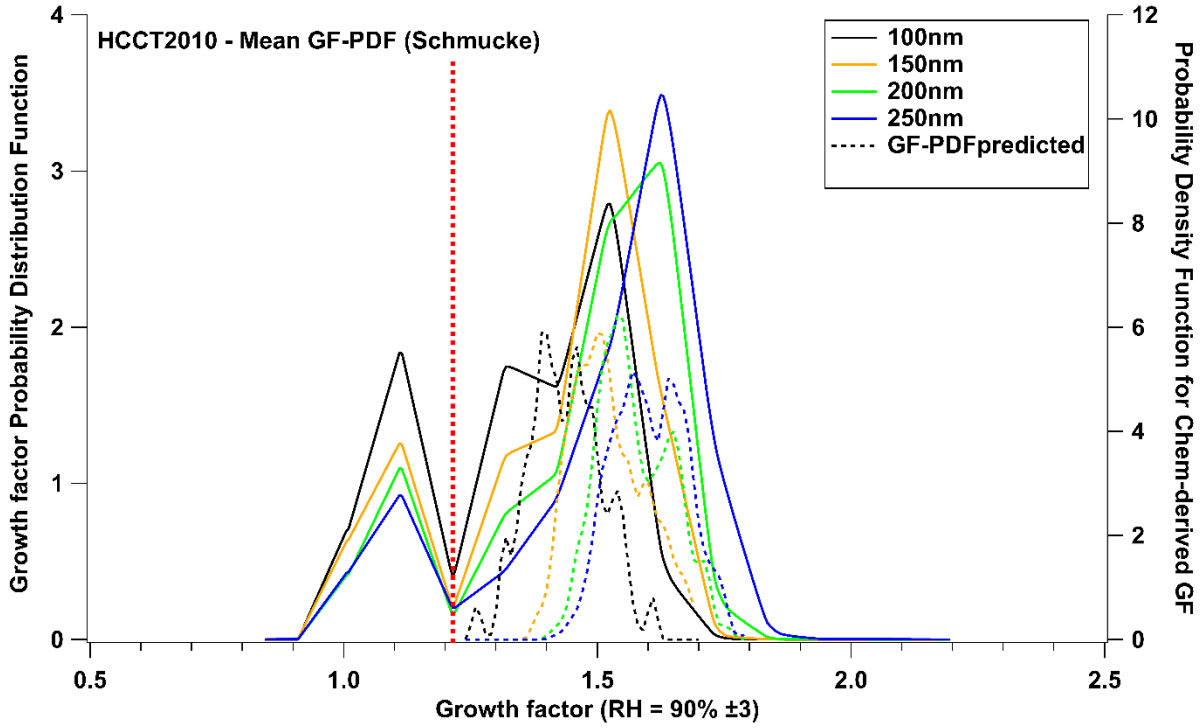

Figure S10. The mean GF-PDFs for the HCCT 2010 campaign at Schmücke.

Table S1. Mean/Median values for the whole period

Diameters	**100**	**150**	**200**	**250**
GF	1.41	1.49	1.55	1.58
$\kappa_{measured}$	0.24	0.29	0.35	0.36
κ_{chem} **κ_{org} = 0.1**	0.21	0.21	0.21	0.22
κ_{chem} **κ_{org} = 0.2**	0.348	0.349	0.35	0.35
F1-mean	0.24	0.17	0.15	0.15
F1-minimum	0	0	0	0
F1-maximum	1	1	0.9	0.9
F2-mean	0.75	0.82	0.84	0.84
F2-minimum	0	0	0.09	0.01
F2-maximum	1	1	1	1

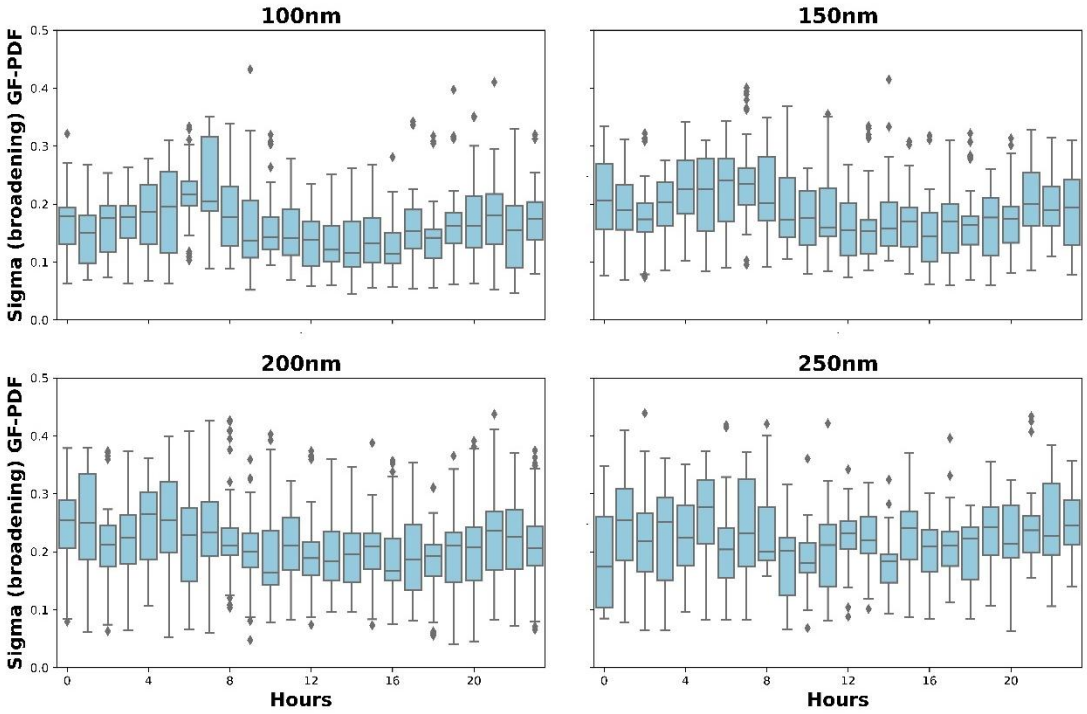

Figure S11. Diurnal Percentiles of the standard deviation σ for each dry size

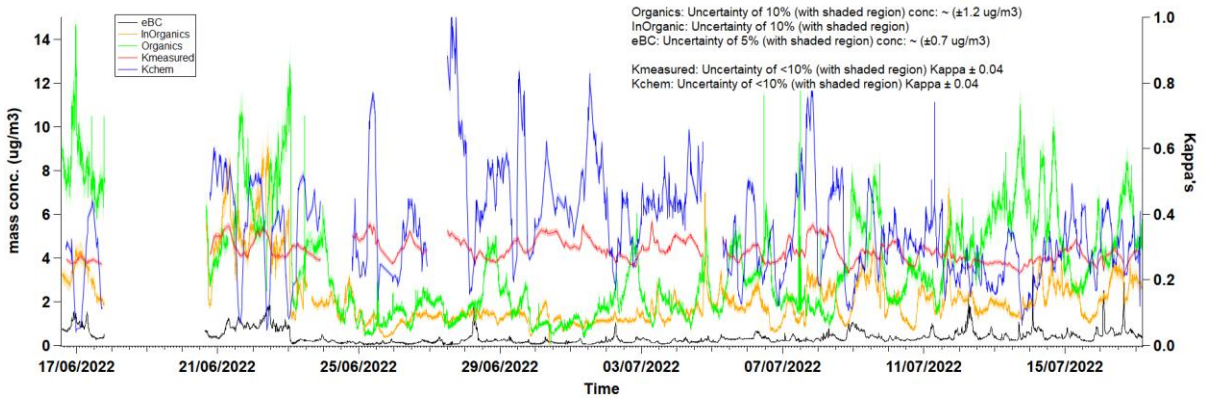

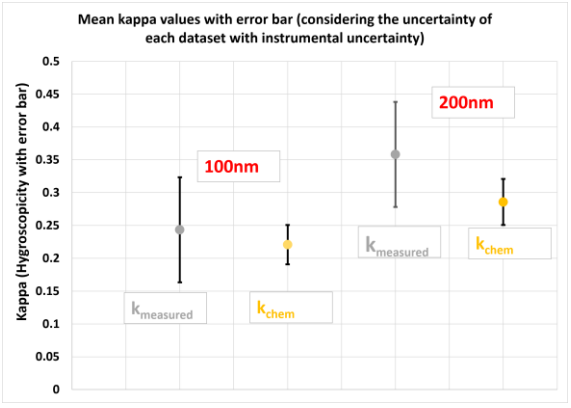

Figure S12. Showing the uncertainty for chemical composition, hygroscopicity Kappa's (here for dia:200nm), and BC measurement (top); the mean kappa with error bar to show the uncertainty for each dataset for 100 & 200nm (bottom).

The standard deviation and combined uncertainty method is used to calculate the uncertainty. For PNSD, uncertainty for each size is calculated. All files are attached in the supplementary folder.

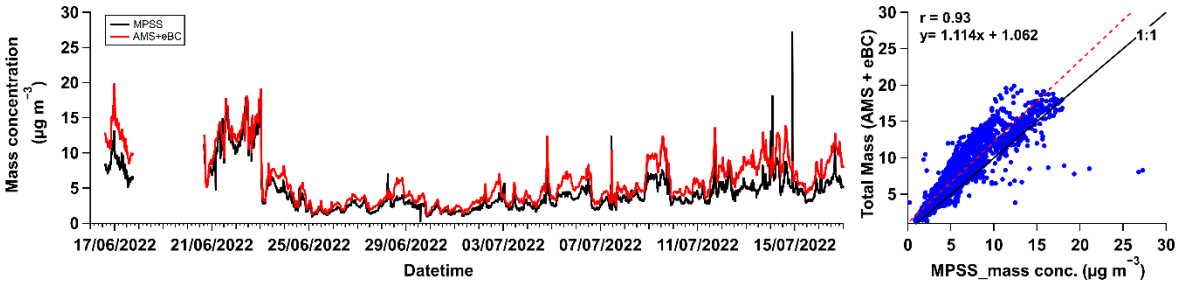

Figure S13. The mass closure for data quality checks with MPSS and AMS + BC mass concentrations.

The total mass concentrations (AMS+BC) are calculated, and density correction is applied with the effective density (ρ) of individual species (Org, NO3, SO4, NH4, Cl and BC) from literature (Park et al., 2004; Kondo et al., 2011; Poulain et al., 2014). The agreement between mass concentration from both instruments is correlated (r = 0.93) with a slope of y = 1.11x + 1.06, which is suitable for data quality.

Reference

Kondo, Y., Sahu, L., Moteki, N., Khan, F., Takegawa, N., Liu, X., Koike, M., and Miyakawa, T.: Consistency and Traceability of Black Carbon Measurements Made by Laser-Induced Incandescence, Thermal-Optical Transmittance, and Filter-Based Photo-Absorption Techniques, Aerosol Sci. and Techno., 45, 295–312, https://doi.org/10.1080/02786826.2010.533215, 2011.

Sjogren, S., Gysel, M., Weingartner, E., Alfarra, M. R., Duplissy, J., Cozic, J., Crosier, J., Coe, H., and Baltensperger, U.: Hygroscopicity of the submicrometer aerosol at the high-alpine site Jungfraujoch, 3580 m a.s.l., Switzerland, Atmos. Chem. Phys., 8, 5715–5729, https://doi.org/10.5194/acp-8-5715-2008, 2008.

Spitieri, C., Gini, M., Gysel-Beer, M., and Eleftheriadis, K.: Annual cycle of hygroscopic properties and mixing state of the suburban aerosol in Athens, Greece, Atmos. Chem. Phys., 23, 235–249, https://doi.org/10.5194/acp-23-235-2023, 2023.

Park, K., Kittelson, D. B., Zachariah, M. R., and McMurry, P. H.: Measurement of inherent material density of nanoparticle agglomerates, J. Nanopart. Res, 6, 267–272, https://doi.org/10.1023/B:NANO.0000034657.71309.e6, 2004.

Poulain, L., Birmili, W., Canonaco, F., Crippa, M., Wu, Z. J., Nordmann, S., Spindler, G., Prévôt, A. S. H., Wiedensohler, A., and Herrmann, H.: Chemical mass balance of 300 °c non-volatile particles at the tropospheric research site Melpitz, Germany, Atmos Chem Phys, 14, 10145–10162, https://doi.org/10.5194/ACP-14-10145-2014, 2014.